Property Integration: Componentless Design Techniques and Visualization Tools

Mahmoud M. El-Halwagi, Ian M. Glasgow, and Xiaoyun Qin
Chemical Engineering Dept., Texas A&M University, College Station, TX 77843

Mario R. Eden
Dept. of Chemical Engineering, Auburn University, Auburn, AL 36849

DOI 10.1002/aic.10305
Published online in Wiley InterScience (www.interscience.wiley.com).

Standard techniques for process design are based on tracking individual chemical species. Component material balances are at the heart of any design approach. Nonetheless, many design problems are not component dependent, but are driven by properties. Recently, the concept of clustering has been introduced to enable the conserved tracking of surrogate properties. Hence, the process design can be optimized, based on integrating properties instead of chemical species. Systematic techniques have been developed for this new paradigm of property integration *to illustrate its applicability. Property integration is defined as a functionality-based, holistic approach to the allocation and manipulation of streams and processing units, which is based on tracking, adjusting, assigning, and matching functionalities throughout the process. Revised lever arm rules are devised to allow optimal allocation while maintaining intra- and interstream conservation of the property-based clusters. The property integration problem is mapped into the cluster domain. This dual problem is solved in terms of clusters and then mapped to the primal problem in the property domain. Several new rules are derived for graphical techniques. Particularly, systematic rules and visualization techniques for the identification of optimal mixing of streams and their allocation to units. Furthermore, a derivation of the correspondence between clustering arms and fractional contribution of streams is presented. This correspondence is employed to minimize the usage of fresh resources by minimizing cluster arms. The selection of optimal values of the augmented property index is also developed. Finally, graphical tools are devised for task identification of property adjustment. The new techniques are illustrated using a case study on fiber recovery in papermaking.* *AIChE J,* 50: 1854–1869, 2004
Keywords: property clusters, visualization, functionality driven design, process integration, snythesis

Introduction

Over the past two decades, process integration has witnessed significant progress in the development of systematic methodologies, tools, and applications. Particularly, two main branches of process integration have been developed: energy integration and mass integration. Energy integration focuses on the system-level optimization of heat, power, fuel, and utilities (for example, Linnhoff et al., 1994). However, mass integration is a holistic approach to the allocation, separation, and generation of streams and species throughout the process (for example, El-Halwagi and Spriggs, 1998; El-Halwagi, 1997). Mass

Correspondence concerning this article should be addressed to M. M. El-Halwagi at El-Halwagi@TAMU.edu.
Current address of I. M. Glasgow: Chemical Engineering Dept., Ecole Polytechnique, P. O. Box 6979, Station Centre-ville, Montreal, Qeubec, Canada; email: ian-michael.glasgow@polymtl.ca.

integration and, consequently, process design has always been carried out on the basis of chemical components. Therefore, tracking, manipulation, and allocation of species are key design tools, starting with component material balances to process modeling equations that are based on targeted species. However, should components always constitute the basis for process design and optimization? Interestingly enough, the answer is no! Many process units are designed to accept or yield certain properties of the streams regardless of the chemical constituents. For instance, the design and performance of a papermaking machine is based on properties (for example, reflectivity, opacity, and density, to name a few). A heat exchanger performs based on the heat capacities and heat-transfer coefficients of the matched streams. The chemical identity of the components is only useful to the extent of determining the values of heat capacities and heat-transfer coefficients. Similar examples can be given for many other units (for example, vapor pressure in condensers, specific gravity in decantation, relative volatility in distillation, Henry's coefficient in absorption, density and head in pumps, density, pressure ratio, and heat-capacity ratio in compressors, and so on).

Since properties (or functionalities) form the basis of performance of many units, it will be very insightful to develop design procedures based on key properties instead of key compounds. The challenge, however, is that while chemical components are conserved, properties are not. Therefore, the question is: whether or not it is possible to track these functionalities instead of compositions? The answer is yes! Recent work done by Shelley and El-Halwagi (2000) has shown that it is possible to tailor conserved quantities, called clusters, that act as surrogate properties, and enable the conserved tracking of functionalities instead of components.

The essence of the componentless approach is to develop conserved quantities called clusters that are related to the nonconserved properties. The basic mathematical expressions for clusters are given by Shelley and El-Halwagi (2000), and are summarized in the following section. Suppose that we have N_s streams. Each stream s is characterized by N_C raw properties. Consider, the class of properties whose mixing rules for each raw property are given by the following equation

$$\psi_i(\bar{p}_i) = \sum_{s=1}^{N_s} x_s \psi_i(p_{i,s}) \tag{1}$$

where x_s is the fractional contribution of the s^{th} stream into the total flow rate of the mixture and $\psi_i(p_{i,s})$ is an operator on $p_{i,s}$ which can be normalized into a dimensionless operator by dividing by a reference value

$$\Omega_{i,s} = \frac{\psi_i(p_{i,s})}{\psi_i^{\text{ref}}} \tag{2}$$

Then, an augmented property index (AUP) for each stream s is defined as the summation of the dimensionless raw property operators

$$AUP_s = \sum_{i=1}^{N_C} \Omega_{i,s} \quad s = 1, 2, \ldots, N_s \tag{3}$$

The cluster for property i in stream s, $C_{i,s}$, is defined as follows

$$C_{i,s} = \frac{\Omega_{i,s}}{AUP_s} \tag{4}$$

Therefore, one can show intra-stream conservation for clusters. In other words, for any stream s, the sum of clusters must be conserved adding up to a constant (for example, unity), that is

$$\sum_{i=1}^{N_C} C_{i,s} = 1 \quad s = 1, 2, \ldots, N_s \tag{5}$$

Let the cluster arm be defined as

$$\beta_s = \frac{x_s AUP_s}{\overline{AUP}} \tag{6}$$

where

$$\overline{AUP} = \sum_{s=1}^{N_s} x_s AUP_s \tag{7}$$

Therefore, one can show inter-stream conservation upon mixing, which implies that

$$\bar{C}_i = \sum_{s=1}^{N_s} \beta_s C_{i,s} \quad i = 1, 2, \ldots, N_C \tag{8}$$

where $\bar{C}_i$ is the mean cluster resulting from adding the individual clusters of N_s streams. Inter-stream conservation allows for lever-arm mixing rules to apply to the system. Lever arm rules are consistent additive rules for the system. Although the mixing of the original properties may be based on nonlinear rules, the clusters are tailored to exhibit linear mixing rules in the cluster domain. When two sources (s and $s+1$) are mixed, the locus of all mixtures on the cluster ternary diagram is given by the straight line connecting sources s and $s+1$. Depending on the fractional contributions of the streams, the resulting mixture splits the mixing line in ratios β_s and β_{s+1}. Similarly, when N_s sources are mixed, the attainable cluster region is enclosed by the polygon (N_s vertices) connecting the sources.

The aforementioned intra- and inter-stream conservation characteristics enable the visual tracking of clusters and can provide unique insights into design from the perspective of properties. Notwithstanding, the novel concepts and usefulness of the work of Shelley and El-Halwagi (2000), it has several limitations:

- Property alteration via condensation: The problem statement is limited to streams whose properties can be altered only by condensation devices (simple functions of temperature and pressure). Clearly, there are numerous processing devices that can be used to modify the desired properties and their performance is much more complex than a simple dependence on temperature and pressure.
- Mapping of infinite points from the property domain to the cluster domain: In order to visualize the feasibility region for

each process sink on the cluster domain, we have to map each point from the feasibility region on the property domain to the corresponding cluster.

- Optimization by enumeration: Although the visualization tools give bounds on the feasible solution, they do not directly identify optimal blends. Instead, within the feasibility region, the costs of several mixtures are assessed, compared, and the optimum solution is chosen from among the enumerated alternatives.

In this article, we overcome all of the abovementioned limitations and address the more general problem of integrating properties of streams and units. We define this new paradigm of "*property integration*" as a functionality-based holistic approach to the allocation and manipulation of streams and processing units, which is based on functionality tracking, adjustment, and assignment throughout the process. In particular this article provides the following new contributions:

- Address a general problem of allocating sources to sinks and modifying their properties using any interception devices.
- Develop the mathematical expressions that define the exact shape of the feasibility region on the cluster domain using a finite number of points that can be determined *a priori*, and without enumeration.
- Derive rigorous optimization rules and associated mathematical expressions that define optimal blends, allocation strategies, and tasks of property-modifying devices.

The visualization tools associated with the derived rules will be presented. Finally, a case study on fiber recovery in papermaking will be addressed to show the validity of the new approach.

Problem Statement

The overall problem to be addressed can be stated as follows: "Given a process with certain sources (streams) and sinks (units) along with their properties and constraints, it is desired to develop graphical techniques that identify optimum strategies for allocation and interception that integrate the properties of sources, sinks, and interceptors so as to optimize a desirable process objective (for example, minimum usage of fresh resources, maximum utilization of process resources, minimum cost of external streams) while satisfying the constraints on properties and flow rate for the sinks".

The problem can be more formally stated as follows: Given is a set of sources: SOURCES $= \{s|s=1,N_s\}$. These sources are classified into two categories: a number N_{internal} of internal (process) streams whose flow rates are bound by their availability in the process, and a number N_{external} of external streams whose cost per unit mass is Cost_s. Each source s is characterized by a set of properties: $\text{PROP}_s = \{p_{i,s}|\ i=1,N_C\}$. Given also is a set of sinks or process units: SINKS $= \{u|u=1,N_{\text{Sinks}}\}$. Each sink has constraints on the properties and flow rate of its feed, that is

$$p_{i,u}^{\min} \le \text{property } i \text{ of feed to sink } u \le p_{i,u}^{\max} \quad i = 1, 2, \ldots, N_C \text{ and } u = 1, 2, \ldots, N_{\text{Sinks}} \quad (9)$$

and

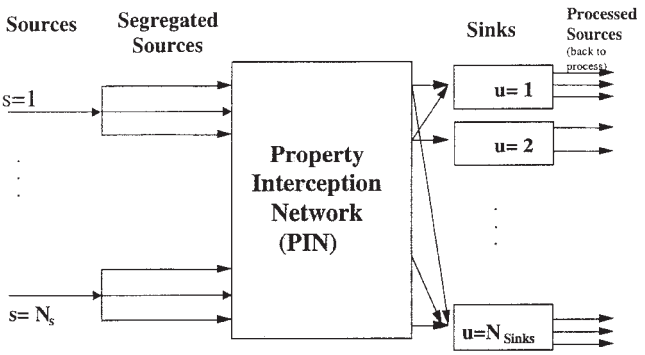

Figure 1. Allocation and interception framework for property integration.

$$F_u^{\min} \le \text{Flow rate of feed to sink } u \le F_u^{\max} \quad u = 1, 2, \ldots, N_{\text{Sinks}} \quad (10)$$

Our objective is to develop visualization tools that systematically optimize a certain process objective (for example, minimum usage of fresh resources, maximum utilization of process resources, minimum cost of external streams) while satisfying the constraints on properties and flow rate for the sinks.

As shown by Figure 1, the solution strategies include a combination of allocation and interception. Allocation of sources involves the segregation and mixing of streams and their assignment to units throughout the process. Interception involves the use of processing units (typically new equipment) to adjust the properties of the various streams. If no capital investment is available for new interception devices, then a no/low cost solution will be based on the allocation of external sources and the recycle/reuse of internal sources to meet the constraints of the sinks.

In order to address the aforementioned problem, the following design decisions must be made:

- What is the exact shape of the feasibility region for each sink?
- What is the optimal allocation of each process stream (what flow rate should be used? where should it go?)?
- How much external sources should be used? Where?
- What are the segregation and mixing needs?
- Is interception needed to adjust the properties of the sources? What are the optimal interception tasks to reach process targets or objectives?.

The following section presents a systematic framework for addressing the aforementioned problem. Derivation of optimization rules, as well as graphical tools will be developed.

Theoretical Analysis

Determination of boundaries of the feasible region (BFR)

As stated earlier, exact mapping of the feasibility region from the property domain to the cluster domain entails the conversion of an infinite number of feasible points. Instead, it is highly desirable to identify the exact shape of the feasibility region without enumeration. For an accurate representation of the feasibility region, two questions arise:

• What is the minimum number of boundary lines defining the feasibility region?

• What are the mathematical expressions for the vertices and lines constituting the BFR?.

The following mathematical analysis answers these questions, and establishes the exact expressions for the BFR *a priori* and without enumeration.

Consider a cluster of stream "s" fed to a unit "u" with three targeted properties*: i, j*, and *k*. According to the definition of clusters given by Eq. 4, we have

$$C_{i,s} = \frac{\Omega_{i,s}}{\Omega_{i,s} + \Omega_{j,s} + \Omega_{k,s}} = \frac{1}{1 + \dfrac{\Omega_{j,s}}{\Omega_{i,s}} + \dfrac{\Omega_{k,s}}{\Omega_{i,s}}} \tag{11}$$

$$C_{j,s} = \frac{\Omega_{j,s}}{\Omega_{i,s} + \Omega_{j,s} + \Omega_{k,s}} = \frac{1}{\dfrac{\Omega_{i,s}}{\Omega_{j,s}} + 1 + \dfrac{\Omega_{k,s}}{\Omega_{j,s}}} \tag{12}$$

$$C_{k,s} = \frac{\Omega_{k,s}}{\Omega_{i,s} + \Omega_{j,s} + \Omega_{k,s}} = \frac{1}{\dfrac{\Omega_{i,s}}{\Omega_{k,s}} + \dfrac{\Omega_{j,s}}{\Omega_{k,s}} + 1} \tag{13}$$

Therefore,

$$C_{i,s}^{\max} = \frac{1}{1 + \dfrac{\Omega_{j,s}^{\min}}{\Omega_{i,s}^{\max}} + \dfrac{\Omega_{k,s}^{\min}}{\Omega_{i,s}^{\max}}} \tag{14}$$

where $\Omega_{i,s}^{\max}$, $\Omega_{j,s}^{\min}$, and $\Omega_{k,s}^{\min}$ are the maximum, minimum, and minimum feasible values of, $\Omega_{i,s}$, $\Omega_{j,s}$, and $\Omega_{k,s}$, respectively. These are readily calculated values from the property domain. For instance, consider a sink *u*, whose constraints for property *i* are given by Eq. 9. Suppose we have a property operator ψ_i, which is monotonically increasing with the raw property $p_{i,s}$. Then

$$\Omega_{i,s}^{\min} = \frac{\psi_i(p_{i,u}^{\min})}{\psi_i^{\text{ref}}} \tag{15}$$

and

$$\Omega_{i,s}^{\max} = \frac{\psi_i(p_{i,u}^{\max})}{\psi_i^{\text{ref}}} \tag{16}$$

Similarly

$$C_{i,s}^{\min} = \frac{1}{1 + \dfrac{\Omega_{j,s}^{\max}}{\Omega_{i,s}^{\min}} + \dfrac{\Omega_{k,s}^{\max}}{\Omega_{i,s}^{\min}}} \tag{17}$$

The same analysis can be carried out for properties *j* and *k*, leading to

$$C_{j,s}^{\max} = \frac{1}{\dfrac{\Omega_{i,s}^{\min}}{\Omega_{j,s}^{\max}} + 1 + \dfrac{\Omega_{k,s}^{\min}}{\Omega_{j,s}^{\max}}} \tag{18}$$

$$C_{j,s}^{\min} = \frac{1}{\dfrac{\Omega_{i,s}^{\max}}{\Omega_{j,s}^{\min}} + 1 + \dfrac{\Omega_{k,s}^{\max}}{\Omega_{j,s}^{\min}}} \tag{19}$$

$$C_{k,s}^{\max} = \frac{1}{\dfrac{\Omega_{i,s}^{\min}}{\Omega_{k,s}^{\max}} + \dfrac{\Omega_{j,s}^{\min}}{\Omega_{k,s}^{\max}} + 1} \tag{20}$$

$$C_{k,s}^{\min} = \frac{1}{\dfrac{\Omega_{i,s}^{\max}}{\Omega_{k,s}^{\min}} + \dfrac{\Omega_{j,s}^{\max}}{\Omega_{k,s}^{\min}} + 1} \tag{21}$$

Our strategy for identifying the BFR will start by determining an overestimation of the feasibility region, followed by an underestimation of the feasibility region, then identifying the BFR in the middle region. Consider a ternary cluster diagram with the vertices C_i, C_j, and C_k.

The overestimating line parallel to the C_j and C_k has a value of the i^{th} coordinate equal to $C_{i,s}^{\max}$, as given by Eq. 14. On this overestimating line, we can identify one feasible point with $\Omega_{i,s} = \Omega_{i,s}^{\max}$, $\Omega_{j,s} = \Omega_{j,s}^{\min}$, $\Omega_{k,s} = \Omega_{k,s}^{\min}$ which corresponds to the following cluster point

$$\left(\frac{\Omega_{i,s}^{\max}}{\Omega_{i,s}^{\max} + \Omega_{j,s}^{\min} + \Omega_{k,s}^{\min}}, \frac{\Omega_{j,s}^{\min}}{\Omega_{i,s}^{\max} + \Omega_{j,s}^{\min} + \Omega_{k,s}^{\min}}, \frac{\Omega_{k,s}^{\min}}{\Omega_{i,s}^{\max} + \Omega_{j,s}^{\min} + \Omega_{k,s}^{\min}} \right) \tag{22}$$

Since this is a feasible point that lies on the overestimator of the BFR, then it must also lie on the BFR itself. Similarly, we can identify a feasible point on each of the five other overestimating lines. Each of these points is characterized by a combination of minimum and maximum values of the dimensionless operators (Ω's). The six feasible points on the overestimating lines are shown in Figure 2a.

Consider a mixture of two feasible points with the resulting mixture satisfying the sink constraints. Using the cluster representation, the mixture lies on the straight line connecting the two feasible points. This straight line is contained within the feasibility region and, therefore, is an underestimator for the BFR. Similarly, we can connect the six feasible points that lie on the BFR to generate an underestimator for the BFR as shown in Figure 2b.

Now that we have bounded the BFR between an overestimator and an underestimator, we can identify additional points on the BFR. One way of identifying additional points on the

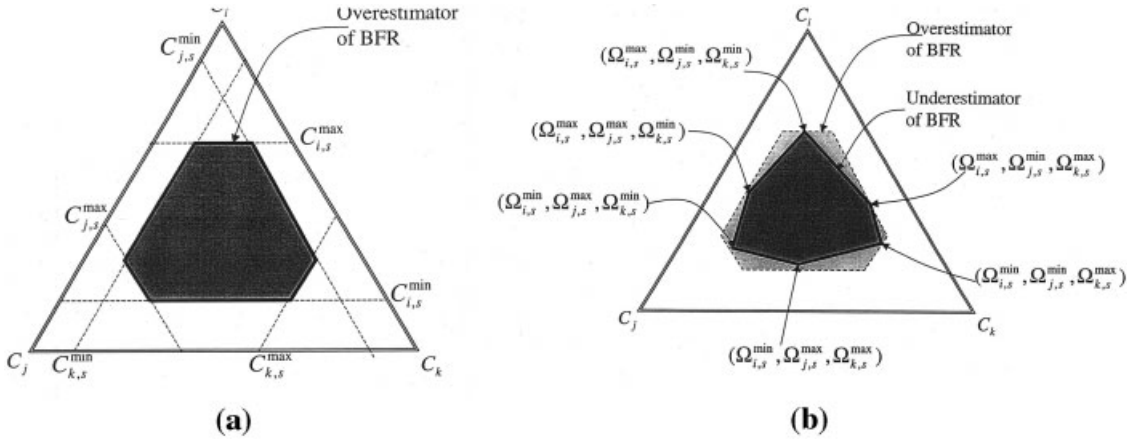

Figure 2. Overestimation of the BRF. Underestimation of the BRF.

BFR is to extend the underestimating lines to a vertex, then identify the line with maximum (or minimum) slope which passes through a feasible point. This feasible point will lie on the BFR. The collection of all these identified feasible points on the BFR constitutes the BFR. In order to carry out this search involving maximum and minimum slopes, it is convenient to transform the ternary cluster coordinates in Cartesian coordinate, as can be seen from Figure 3

$$Y_s = \left(\sin\frac{\pi}{3}\right)C_{i,s} = 0.866C_{i,s} = \frac{0.866\Omega_{i,s}}{\Omega_{i,s}+\Omega_{j,s}+\Omega_{k,s}} \quad (23)$$

$$X_s = 1 - C_{j,s} - \left(\cos\frac{\pi}{3}\right)C_{i,s} = 1 - C_{j,s} - 0.500C_{i,s} = \frac{0.500\Omega_{i,s}+\Omega_{k,s}}{\Omega_{i,s}+\Omega_{j,s}+\Omega_{k,s}} \quad (24)$$

Let us start with two points on the BFR. For instance consider the two points characterized by $(\Omega_{i,s}^{\min}, \Omega_{j,s}^{\min}, \Omega_{k,s}^{\max})$ and $(\Omega_{i,s}^{\min}, \Omega_{j,s}^{\max}, \Omega_{k,s}^{\max})$. The slope of the line connecting these two points is given by

$$\text{Slope} = \frac{\dfrac{0.866\Omega_{i,s}^{\min}}{\Omega_{i,s}^{\min}+\Omega_{j,s}^{\min}+\Omega_{k,s}^{\max}} - \dfrac{0.866\Omega_{i,s}^{\min}}{\Omega_{i,s}^{\min}+\Omega_{j,s}^{\max}+\Omega_{k,s}^{\max}}}{\dfrac{0.500\Omega_{i,s}^{\min}+\Omega_{k,s}^{\max}}{\Omega_{i,s}^{\min}+\Omega_{j,s}^{\min}+\Omega_{k,s}^{\max}} - \dfrac{0.500\Omega_{i,s}^{\min}+\Omega_{k,s}^{\max}}{\Omega_{i,s}^{\min}+\Omega_{j,s}^{\max}+\Omega_{k,s}^{\max}}} = \frac{1.732}{1.000+2*\dfrac{\Omega_{k,s}^{\max}}{\Omega_{i,s}^{\min}}} \quad (25)$$

The intercept of this line is obtained from the slope and one point on the line, that is

$$\text{Intercept} = \frac{0.866\Omega_{i,s}^{\min}}{\Omega_{i,s}^{\min}+\Omega_{j,s}^{\min}+\Omega_{k,s}^{\max}} - \left(\frac{1.732}{1.000+2*\dfrac{\Omega_{k,s}^{\max}}{\Omega_{i,s}^{\min}}}\right) \times \left(\frac{0.500\Omega_{i,s}^{\min}+\Omega_{k,s}^{\max}}{\Omega_{i,s}^{\min}+\Omega_{j,s}^{\min}+\Omega_{k,s}^{\max}}\right) = 0.000 \quad (26)$$

Since the origin coordinates are located at ($C_i = 0$, $C_j = 1$, $C_k = 0$), which correspond to ($Y = 0$, $X = 0$), then the zero intercept indicates that this straight line connecting the two feasible points passes through the origin.

The same result can be obtained by deriving the slope equation for any line emanating from a vertex point whose Cartesian coordinates are designated as ($\bar{Y}_\nu$, $\bar{X}_\nu$), with the origin located at ($C_i = 0$, $C_j = 1$, $C_k = 0$). By moving the coordinates to the ν^{th} vertex, the slope of any line emanating from the vertex coordinates ($\bar{Y}_\nu$, $\bar{X}_\nu$) is described by

$$\text{Slope}_{\text{From}(\bar{Y}_\nu,\bar{X}_\nu)} = \frac{0.866C_i - \bar{Y}_\nu}{1 - C_j - 0.500C_i - \bar{X}_\nu} \quad (27)$$

where (C_i, C_j, and C_k) is any point lying on the line emanating from the ν^{th} vertex. Let us substitute for the clusters in terms of omegas

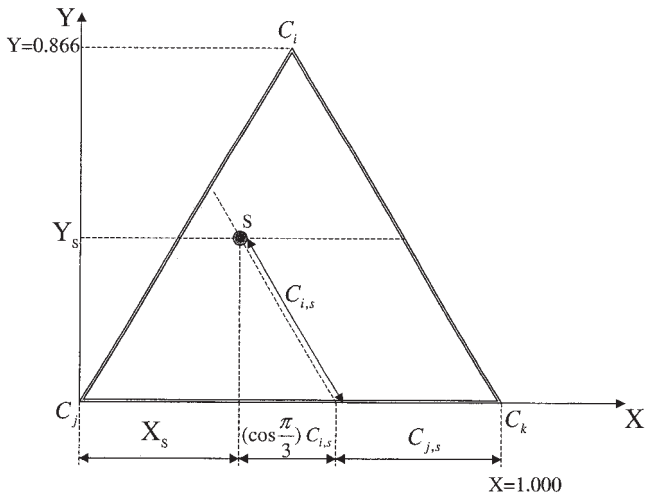

Figure 3. Relationship between ternary coordinates and cartisian coordinates.

$$\text{Slope}_{\text{From}(\bar{Y}_\nu,\bar{X}_\nu)} = \frac{0.866\Omega_i - \bar{Y}_\nu\Omega_i - \bar{Y}_\nu\Omega_j - \bar{Y}_\nu\Omega_k}{\Omega_i + \Omega_j + \Omega_k - \Omega_j - 0.500\Omega_i - \bar{X}_\nu\Omega_i - \bar{X}_\nu\Omega_j - \bar{X}_\nu\Omega_k}$$

$$= \frac{(0.866 - \bar{Y}_\nu) * \Omega_i - \bar{Y}_\nu\Omega_j - \bar{Y}_\nu\Omega_k}{(0.500 - \bar{X}_\nu) * \Omega_i - \bar{X}_\nu\Omega_j + (1 - \bar{X}_\nu)\Omega_k} \quad (28)$$

or

$$[(0.500 - \bar{X}_\nu) * \text{Slope}_{\text{From}(\bar{Y}_\nu,\bar{X}_\nu)} - 0.866 + \bar{Y}_\nu]\Omega_i + (\bar{Y}_\nu - \bar{X}_\nu * \text{Slope}_{\text{From}(\bar{Y}_\nu,\bar{X}_\nu)})\Omega_j + [(1.000 - \bar{X}_\nu) * \text{Slope}_{\text{From}(\bar{Y}_\nu,\bar{X}_\nu)} - \bar{Y}_\nu]\Omega_k = 0.000 \quad (29)$$

Let us again consider the two points on the BFR characterized by $(\Omega_{i,s}^{\min}, \Omega_{j,s}^{\min}, \Omega_{k,s}^{\max})$ and $(\Omega_{i,s}^{\min}, \Omega_{j,s}^{\max}, \Omega_{k,s}^{\max})$. We note that the two values $\Omega_{i,s}^{\min}$ and $\Omega_{k,s}^{\max}$ are common for both points, and, therefore, the slope for the line connecting these two points is determined by $\Omega_{i,s}^{\min}$ and $\Omega_{k,s}^{\max}$ only, and not $\Omega_{j,s}$. Indeed, while $\Omega_{i,s}^{\min}$ and $\Omega_{k,s}^{\max}$ determine the slope of the line, different values of $\Omega_{j,s}$ give different points on the line. Therefore, for the slope to be independent of $\Omega_{j,s}$, the coefficient of $\Omega_{j,s}$ in the slope equation is set to zero, that is

$$\bar{Y}_\nu = 0 \quad \text{and} \quad \bar{X}_\nu = 0 \quad (30)$$

This is the same result obtained earlier. However, the equation for the slope of any line emanating from this vertex ($\bar{Y}_\nu = 0$, $\bar{X}_\nu = 0$) or ($C_i = 0$, $C_j = 1$, $C_k = 0$) is given by

$$\text{Slope}_{\text{From}(0,1,0)} = \frac{0.866\Omega_{i,s}}{\Omega_{i,s} + \Omega_{j,s} + \Omega_{k,s} - \Omega_{j,s} - 0.500\Omega_{i,s}} = \frac{1.732}{1.000 + 2 * \dfrac{\Omega_{k,s}}{\Omega_{i,s}}} \quad (31)$$

Therefore

$$\text{Minimum Slope}_{\text{From}(0,1,0)} = \frac{1.732}{1.000 + 2 * \dfrac{\Omega_{k,s}^{\max}}{\Omega_{i,s}^{\min}}} \quad (32)$$

This is exactly the slope of the line connecting the two points: characterized by $(\Omega_{i,s}^{\min}, \Omega_{j,s}^{\min}, \Omega_{k,s}^{\max})$ and $(\Omega_{i,s}^{\min}, \Omega_{j,s}^{\max}, \Omega_{k,s}^{\max})$ with the result that there are no feasible points between this line and the overestimator. Therefore, the line connecting these two points lies on the actual boundaries of the true BFR.

The foregoing derivation can be repeated for the other points on the BFR. For instance, consider the two points characterized by $(\Omega_{i,s}^{\max}, \Omega_{j,s}^{\min}, \Omega_{k,s}^{\max})$ and $(\Omega_{i,s}^{\max}, \Omega_{j,s}^{\min}, \Omega_{k,s}^{\min})$. The slope of the line connecting these two points is given by

$$\text{Slope} = \frac{\dfrac{0.866\Omega_{i,s}^{\max}}{\Omega_{i,s}^{\max} + \Omega_{j,s}^{\min} + \Omega_{k,s}^{\max}} - \dfrac{0.866\Omega_{i,s}^{\max}}{\Omega_{i,s}^{\max} + \Omega_{j,s}^{\min} + \Omega_{k,s}^{\min}}}{\dfrac{0.500\Omega_{i,s}^{\max} + \Omega_{k,s}^{\max}}{\Omega_{i,s}^{\max} + \Omega_{j,s}^{\min} + \Omega_{k,s}^{\max}} - \dfrac{0.500\Omega_{i,s}^{\max} + \Omega_{k,s}^{\min}}{\Omega_{i,s}^{\max} + \Omega_{j,s}^{\min} + \Omega_{k,s}^{\min}}} = \frac{-1.732}{1.000 + 2 * \dfrac{\Omega_{j,s}^{\min}}{\Omega_{i,s}^{\max}}} \quad (33)$$

and the intercept is $\bar{Y}_\nu = 0$ and $\bar{X}_\nu = 1.0$ which corresponds to ($C_i = 0$, $C_j = 0$, $C_k = 1$). The same results can be obtained from the characteristic equation of the slope by setting the coefficient of $\Omega_{k,s}$ to zero. However, the equation for the slope of any line emanating from this vertex is given by

$$\text{Slope}_{\text{From}(0,0,1)} = \frac{-0.866\Omega_{i,s}}{0.500\Omega_{i,s} + \Omega_{j,s}} \quad (34)$$

Therefore

$$\text{Minimum Slope}_{\text{From}(0,0,1)} = \frac{-1.732}{1.000 + 2 * \dfrac{\Omega_{j,s}^{\min}}{\Omega_{i,s}^{\max}}} \quad (35)$$

which is the same slope of the line connecting the two points $(\Omega_{i,s}^{\max}, \Omega_{j,s}^{\min}, \Omega_{k,s}^{\min})$ and $(\Omega_{i,s}^{\max}, \Omega_{j,s}^{\min}, \Omega_{k,s}^{\max})$. Therefore, there are no points above this line which belong to the feasible region, making it constitute a portion of the true BFR.

This exercise can be repeated for all the lines connecting the six points lying on the intersection of the overestimating and underestimating regions. The mathematical expressions are shown in Table 1, and the graphical results are shown in Figure 4.

The findings of the foregoing analysis can be summarized by the following important results:

- The BFR can be accurately represented by no more than six linear segments
- When extended, the linear segments of the BFR constitute three convex hulls (cones) with their heads lying on the three vertices of the ternary cluster diagram.
- The six points defining the BFR are determined *a priori* and are characterized by the following values of dimensionless operators "Ω's": $(\Omega_{i,s}^{\min}, \Omega_{j,s}^{\min}, \Omega_{k,s}^{\max})$, $(\Omega_{i,s}^{\min}, \Omega_{j,s}^{\max}, \Omega_{k,s}^{\max})$, $(\Omega_{i,s}^{\min}, \Omega_{j,s}^{\max}, \Omega_{k,s}^{\min})$, $(\Omega_{i,s}^{\max}, \Omega_{j,s}^{\max}, \Omega_{k,s}^{\min})$, $(\Omega_{i,s}^{\max}, \Omega_{j,s}^{\min}, \Omega_{k,s}^{\min})$ and $(\Omega_{i,s}^{\max}, \Omega_{j,s}^{\min}, \Omega_{k,s}^{\max})$.

With the rigorous determination of the BFR, we can now proceed and derive optimization rules. In the following section, we develop the new optimization rules for blending and interception. In particular, we derive visualization techniques and revised lever-arm rules that can be systematically used for

Table 1. Coordinates and Slopes for the BFR

Ternary Coordinates for the Vertex (C_i, C_j, C_k)	Cartesian Coordinates for the Vertex (Y, X)	Equation of Maximum Slope from the Vertex	Two Connecting Points on BFR	Equation for Minimum Slope from the Vertex	Two Connecting Points on BFR
(0.0, 1.0, 0.0)	(0.000, 0.000)	$\frac{1.732}{1.000 + 2 * \frac{\Omega_{k,s}^{\min}}{\Omega_{i,s}^{\max}}}$	$(\Omega_{i,s}^{\max}, \Omega_{j,s}^{\min}, \Omega_{k,s}^{\min})$ and $(\Omega_{i,s}^{\max}, \Omega_{j,s}^{\max}, \Omega_{k,s}^{\min})$	$\frac{1.732}{1.000 + 2 * \frac{\Omega_{k,s}^{\max}}{\Omega_{i,s}^{\min}}}$	$(\Omega_{i,s}^{\min}, \Omega_{j,s}^{\max}, \Omega_{k,s}^{\max})$ and $(\Omega_{i,s}^{\min}, \Omega_{j,s}^{\min}, \Omega_{k,s}^{\max})$
(1.0, 0.0, 0.0)	(0.866, 0.500)	$1.732\left(\frac{1 + \frac{\Omega_{j,s}^{\max}}{\Omega_{k,s}^{\min}}}{1 - \frac{\Omega_{j,s}^{\max}}{\Omega_{k,s}^{\min}}}\right)$	$(\Omega_{i,s}^{\max}, \Omega_{j,s}^{\max}, \Omega_{k,s}^{\min})$ and $(\Omega_{i,s}^{\min}, \Omega_{j,s}^{\max}, \Omega_{k,s}^{\min})$	$1.732\left(\frac{1 + \frac{\Omega_{j,s}^{\min}}{\Omega_{k,s}^{\max}}}{1 - \frac{\Omega_{j,s}^{\min}}{\Omega_{k,s}^{\max}}}\right)$	$(\Omega_{i,s}^{\max}, \Omega_{j,s}^{\min}, \Omega_{k,s}^{\max})$ and $(\Omega_{i,s}^{\min}, \Omega_{j,s}^{\min}, \Omega_{k,s}^{\max})$
(0.0, 0.0, 1.0)	(0.000, 1.000)	$\frac{-1.732}{1.000 + 2 * \frac{\Omega_{j,s}^{\max}}{\Omega_{i,s}^{\min}}}$	$(\Omega_{i,s}^{\min}, \Omega_{j,s}^{\max}, \Omega_{k,s}^{\min})$ and $(\Omega_{i,s}^{\min}, \Omega_{j,s}^{\max}, \Omega_{k,s}^{\max})$	$\frac{-1.732}{1.000 + 2 * \frac{\Omega_{j,s}^{\min}}{\Omega_{i,s}^{\max}}}$	$(\Omega_{i,s}^{\max}, \Omega_{j,s}^{\min}, \Omega_{k,s}^{\min})$ and $(\Omega_{i,s}^{\max}, \Omega_{j,s}^{\min}, \Omega_{k,s}^{\max})$

mixing points and property modification tasks. We also derive the optimality conditions for selecting values of the augmented property index of a sink. Graphical tools are then based on these rules.

Relating costs to fractional contribution of sources

Consider two sources (s and $s+1$) that are mixed to satisfy the property constraints of a certain sink. Let x_s and x_{s+1} denote the fractional contributions of the sources s and $s+1$ into the total flow rate of the mixture. Let source s be more expensive than source $s+1$, namely $\text{Cost}_s > \text{Cost}_{s+1}$.

Therefore, the cost of the mixture is given by

$$\begin{aligned}\text{Cost}_{\text{mixture}} &= x_s\text{Cost}_s + (1 - x_s)\text{Cost}_{s+1} \\ &= x_s(\text{Cost}_s - \text{Cost}_{s+1}) + \text{Cost}_{s+1} \quad (36)\end{aligned}$$

Noting that (Cost_s – Cost_{s+1}) is a positive term, therefore, the cost of the mixture is linearly proportional to x_s. Hence, the lower the value of x_s, the lower the cost of the mixture, and we can now deduce the following:

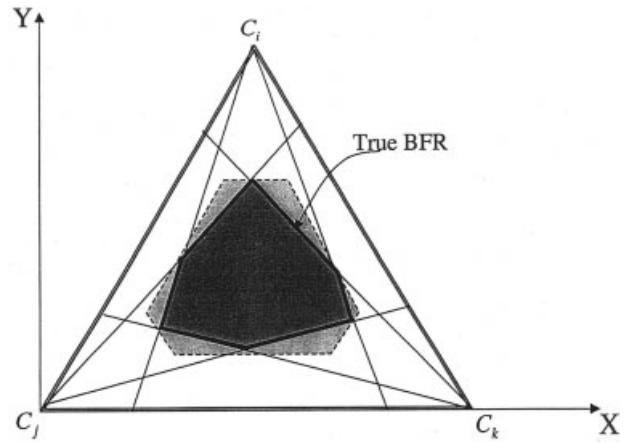

Figure 4. Identification of the true BRF via three convex hulls.

Rule No. 1

When two sources (s and $s+1$) are mixed to satisfy the property constraints of a sink with source s being more expensive than $s+1$, minimizing $\text{Cost}_{mixture}$ is achieved by selecting the minimum feasible value of x_s.

The determination of the feasibility mixing region and selection of the minimum feasible fractional contribution will be determined in the ensuing sections.

Derivation of relationship between minimum cluster arms (β) and minimum fractional contribution

The previous section showed the importance of selecting minimum fractional contribution (x_s). Unfortunately, x_s cannot be directly visualized on the ternary cluster diagram. Instead, the lever arms on the ternary cluster diagram represent another quantity β_s. While x_s represents the fractional contribution of the stream's flow rate to the total flow, β_s has a more subtle meaning. It is necessary to relate both since β_s is the visualization arm on the ternary diagram, but x_s is directly related to the cost of the mixture. The two terms are related through the augmented property index (AUP) as described earlier

$$\beta_s = \frac{x_s AUP_s}{\overline{AUP}} \quad (6)$$

Using Eq. 7, let us rewrite Eq. 6 in the case of mixing two sources (s and $s+1$):

$$\beta_s = \frac{x_s AUP_s}{x_s AUP_s + (1 - x_s)AUP_{s+1}} \quad (37)$$

Rearranging, we get

$$x_s = \frac{\beta_s AUP_{s+1}}{\beta_s AUP_{s+1} + (1 - \beta_s)AUP_s} \quad (38)$$

Next, let's take the first derivative of x_s with respect to β_s.

$$\frac{dx_s}{d\beta_s} = \frac{AUP_{s+1}[\beta_s AUP_{s+1} + (1-\beta_s)AUP_s] - \beta_s AUP_{s+1}[AUP_{s+1} - AUP_s]}{[\beta_s AUP_{s+1} + (1-\beta_s)AUP_s]^2} \tag{39}$$

Rearranging and simplifying, we get

$$\frac{dx_s}{d\beta_s} = \frac{\mathrm{AUP}_s \mathrm{AUP}_{s+1}}{[\beta_s \mathrm{AUP}_{s+1} + (1-\beta_s)\mathrm{AUP}_s]^2} \tag{40}$$

With both AUP_s and AUP_{s+1} being nonnegative, the righthand side of Eq. 40 is also nonnegative. Therefore x_s as a function of β_s, is monotonically increasing. From this, we can state that following rule:

Rule No. 2

On a ternary cluster diagram, minimization of the cluster arm of a source corresponds to minimization of the flow contribution of that source. In other words, ***minimum β_s corresponds to minimum x_s***.

Visualization tools based on rules No. 1 and 2

The two derived rules are important findings, as they allow us to use cluster lever-arm minimization rules (visualized for β_s on the ternary cluster diagram) to correspond to minimum usage of the more expensive source and, consequently, the minimum cost of the mixture. For instance, consider the case of a fresh (external) resource (F) whose flow rate is to be minimized. An example would be raw materials, virgin fibers, fresh solvent, and so on. Let us also consider a process internal stream (W) that can be recycled or reused to reduce the consumption of the more expensive external source. Examples of internal sources include unreacted raw materials, waste streams, spent solvents, and so on. Suppose that it is desired to blend a minimum-cost mixture of the two sources that satisfy the property constraints for the sink to which they are allocated. The feed to the sink is subject to a number of property constraints, which can be mapped to a cluster feasibility region using the clustering mapping equations. Figure 5 shows the internal and external sources, as well as the feasibility region on a ternary cluster source-sink mapping diagram. The straight line connecting the two sources represents the locus for any mixture of W and F. The resulting mixture splits the total mixing arm in the ratios of β_F to β_W. The intersection of the mixing line with the feasibility region of the sink gives the line segment representing all feasible mixtures. This is shown on Figure 5 by the segment connecting points a and c. The question is what should be the optimum mixing point (for example, a, b, or c)? Our objective is to minimize the mixture cost. On the the basis of Rules No. 1 and 2, the optimal mixing point corresponds to the minimum feasible β_F. This is point a as shown on Figure 5. As previously mentioned, this is a necessary condition only. For sufficiency, values of the augmented property index and flow rate should match as well. This issue will be expounded later.

The same concept can be generalized to multiple sources. For instance, consider the mixing of a fresh resource (F) with two internal streams (W_1 and W_2). As can be seen from Figure 6, the mixing zone is bounded by the triangle connecting points F, W_1, and W_2. It is worth noting that the connecting line represents all possible mixtures of W_1 and W_2. If the objective is to minimize the fresh resource, then the optimal mixing point is the one that gives the least ratio of fresh arm to total arm (that is, β_F) as shown on Figure 6.

In case the target for recycling an internal stream (W) is not met, more of the internal stream can be recycled by adjusting its properties via an interception device (for example, separation, reaction, and so on). It is desired to change the properties of W, such that the use of F is minimized. The question is what should be the task of the interception device in altering the properties (and, consequently, the cluster values) of the internal stream? This can be readily determined using graphical techniques. As shown on Figure 7, for the selected mixing point and the desired value of β_F, the fresh arm can be drawn to determine the desired location of the intercepted internal stream (W^{int}). Furthermore, since the values of the augmented property index are known for F and the mixing point of the sink, we can plug the targeted value of x_F into Eq. 7, to calculate the desired value of the augmented property index for W^{int}. Now that the ternary cluster value for W^{int} and its augmented property index have been determined, we can solve the cluster equations backward to calculate the raw properties of W^{int}. This is the minimum extent of interception to achieve maximum recycle of W, or minimum usage of the fresh since additional interception will still lead to the same target of minimum usage, but will result in a mixing point inside the sink and not just on the periphery of the sink. Once the task for

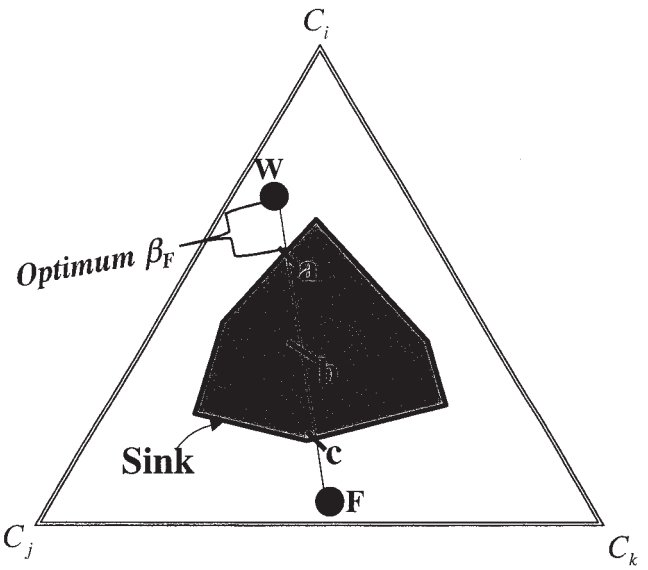

Figure 5. Optimal mixing point for fresh resources (F), and an internal source (w).

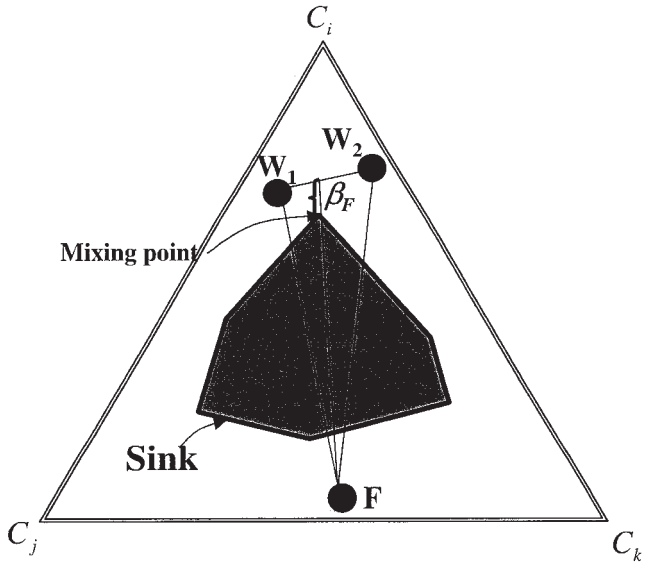

Figure 6. Minimum-arm mixing point for a fresh resource (F).

the interception system is defined, conventional process synthesis techniques can be employed to develop the design and operating parameters for the interception system. The same procedure can be repeated for various mixing points resulting in the task identification of the locus for minimum extent of interception (Figure 8).

Dealing with multiplicity and selection of optimal values of augmented property index

Consider a certain point (combination) on the cluster domain of a sink. Let us refer to this cluster point as (C_1^{sink}, C_2^{sink}, C_3^{sink}). This cluster point may correspond to multiple combinations of property points (points on the BRF are exceptions as they can be uniquely mapped to the property domain. This is attributed to the uniqueness of the six vertices on the BFR. Hence, the

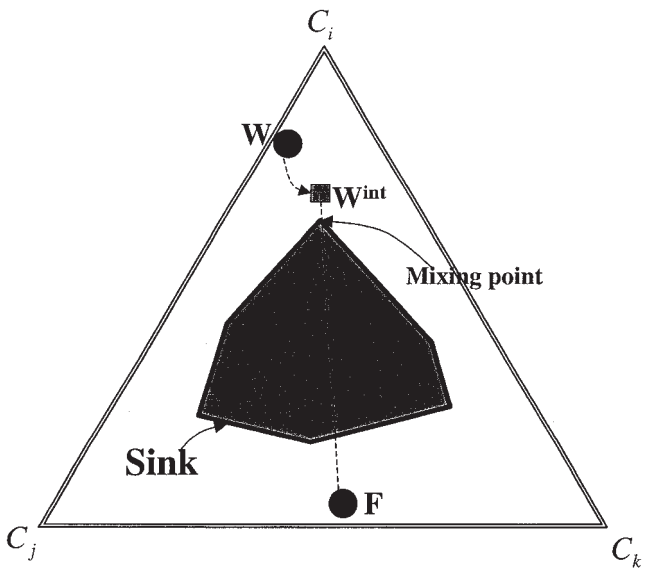

Figure 7. Task identification for the interception system.

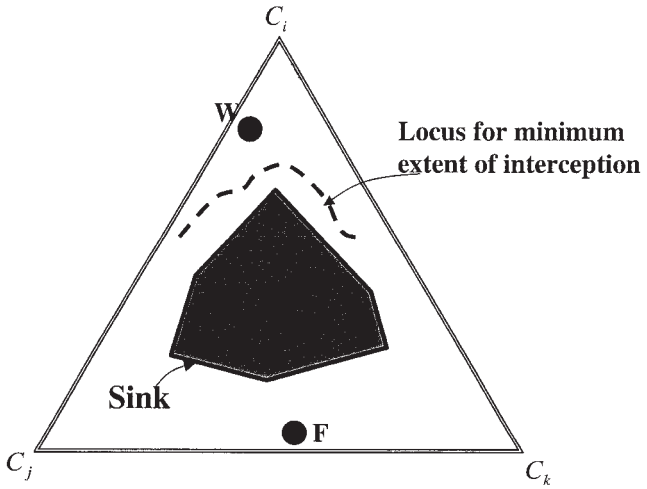

Figure 8. Locus for minimum interception.

lines connecting these vertices (representing mixtures) will also have unique mapping). In other words, as a result of the nonlinear mapping from the property domain to the cluster domain, it is possible to have multiple property points (n_{Multiple}) which belong to the feasible property domain leading to a single value of clusters, that is

$$(C_1^{\text{sink}}, C_2^{\text{sink}}, C_3^{\text{sink}}) \equiv (p_{1,m}, p_{2,m}, p_{3,m}) \tag{41}$$

where $m=1, 2,, n_{\text{Multiple}}$ and $(p1,m, p2,m, p3,m)$ are feasible for the considered sink.

For each property combination ($p_{1,m}$, $p_{2,m}$, $p_{3,m}$), the corresponding augmented property index is referred to as AUP_m. Consequently, we can define the set of all these multiple feasible values of AUP_m as

$$SET\_AUP^{\text{Feasible}}_{(C_1^{\text{sink}},C_2^{\text{sink}},C_3^{\text{sink}})} = \{AUP_m | m = 1, 2, \ldots, n_{\text{Multiple}}\} \tag{42}$$

The range for the values of AUP_m is given by the following interval

$$\text{INTERVAL\_}AUP_m = [\text{Argmin } AUP_m, \text{Argmax } AUP_m] \tag{43}$$

where Argmin AUP_m and Argmax AUP_m are the lowest and highest values of $AUP_m \in SET\_AUP^{\text{Feasible}}_{(C_1^{\text{sink}},C_2^{\text{sink}},C_3^{sink})}$.

As a result of such multiplicity, three conditions must be satisfied to insure feasibility of feeding sources (or mixtures of sources) into a sink:

(1) The cluster value for the source (or mixture of sources) must be contained within the feasibility region of the sink on the cluster ternary diagram.

(2) The values of the augmented property index for the source (or mixture of sources) and the sink must match.

(3) The flow rate of the source (or mixture of sources) must lie within the acceptable feed flow rate range for the sink.

Now, consider that two sources s and $s+1$ are mixed in a ratio of x_s to x_{s+1} to get a mixture whose cluster value matches that of a feasible sink cluster, that is

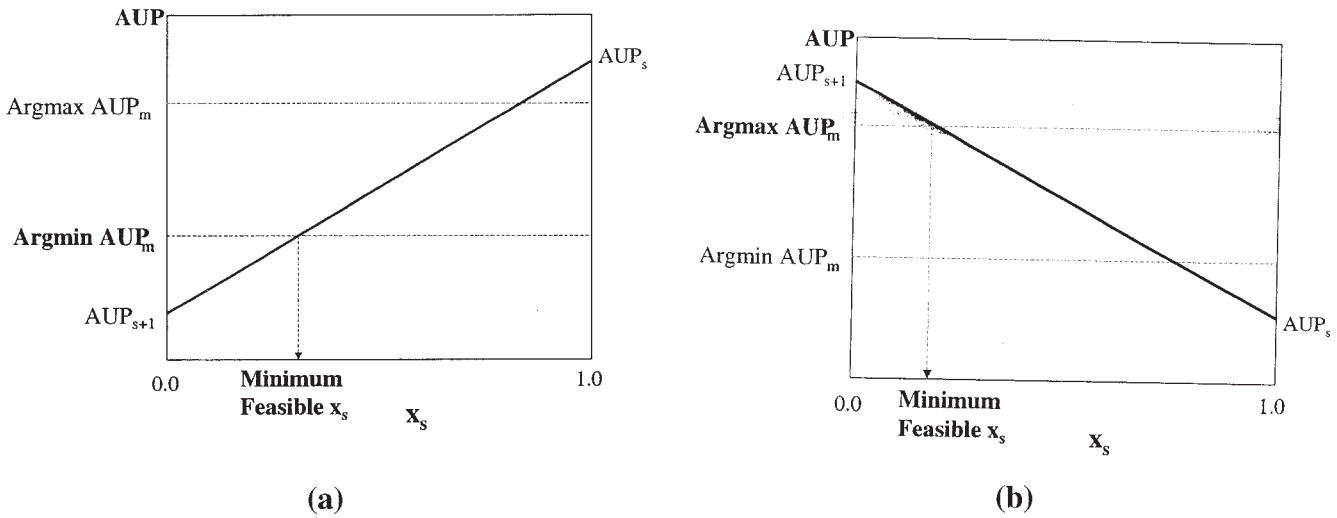

Figure 9. Selection of optimum AUP_m when $AUP_s > AUP_{s+1}$. Selection of optimum AUP_m when $AUP_s < AUP_{s+1}$.

$$(C_1^{\text{mixture}}, C_2^{\text{mixture}}, C_3^{\text{mixture}}) = (C_1^{\text{sink}}, C_2^{\text{sink}}, C_3^{\text{sink}}) \tag{44}$$

It follows from the foregoing discussion that this is a necessary but not sufficient condition for satisfying the sink constraint. In addition to satisfying the previous condition, sufficiency is ensured when the value of the augmented property for the mixture matches a feasible value of the augment property for the sink, that is

$$AUP_{mixture} = AUP_m \in SET\_AUP^{\text{Feasible}}_{(C_1^{\text{sink}}, C_2^{\text{sink}}, C_3^{\text{sink}})} \tag{45}$$

So, which of the n_{Multiple} feasible values of the augmented properties in the set should be selected?

Recalling Rule No. 1, minimizing x_s results in minimizing $\text{Cost}_{\text{mixture}}$. Consequently, we should select an AUP_m, which minimizes x_s. This can be determined by establishing the relationship between AUP_m and x_s.

Let us denote the numerical values of the augmented properties for sources s and $s+1$ as AUP_s and AUP_{s+1}, respectively. These are constants. According to Eq. 7, we can describe the augmented property of the mixture in terms of the individual augmented properties. Substituting into Eq. 45, we get

$$x_s AUP_s + (1 - x_s) AUP_{s+1} = AUP_m \tag{46a}$$

or

$$AUP_m = x_s(AUP_s - AUP_{s+1}) + AUP_{s+1} \tag{46b}$$

Hence

$$x_s = \frac{AUP_m - AUP_{s+1}}{AUP_s - AUP_{s+1}} \tag{47}$$

Therefore

$$\frac{\partial x_s}{\partial AUP_m} = \frac{1}{AUP_s - AUP_{s+1}} \tag{48}$$

which is monotonically increasing if $AUP_s > AUP_{s+1}$, and monotonically decreasing if $AUP_s < AUP_{s+1}$. Therefore, to minimize x_s (and consequently the cost), we should select

$$AUP_m^{\text{optimum}} = \text{Argmin}\, AUP_m \quad \text{if } AUP_s > AUP_{s+1} \tag{49a}$$

$$AUP_m^{\text{optimum}} = \text{Argmax}\, AUP_m \quad \text{if } AUP_s < AUP_{s+1} \tag{49b}$$

These results can be shown graphically in Figures 7a, 9a, and 9b. According to Eq. 46b, the relationship between AUP_m and x_s is represented by a straight line whose slope is $AUP_s - AUP_{s+1}$. If $AUP_s > AUP_{s+1}$, the slope is positive (Figure 9a), which corresponds to Eq. 49a. However, when $AUP_s < AUP_{s+1}$, the slope is negative (Figure 9b), which corresponds to Eq. 49b.

As described by Eq. 46a, the AUP of the sink should match that of the mixture. If no possible mixture can have an AUP matching that selected for the sink (for example, Argmax AUP_m as per Eq. 49a), then we systematically decrease the value of the sink's AUP, starting with Argmax AUP_m, till we get the highest value of AUP_m, which matches that of the mixture. A similar procedure is adopted for the conditions of Eq. 49b, by systematically increasing the value of the sink's AUP, starting with Argmin AUP_m, till we get the highest value of AUP_m, which matches that of the mixture.

Now that the foregoing rules and tools have been developed, we are now in a position to proceed to a case study.

Case Study

To show the power, insights, and practical use of the developed property integration concepts and techniques, we turn our attention to a case study on a papermaking process. Figure 10 is a representation of the process. Wood chips are chemically cooked in a Kraft digester using white liquor (which contains

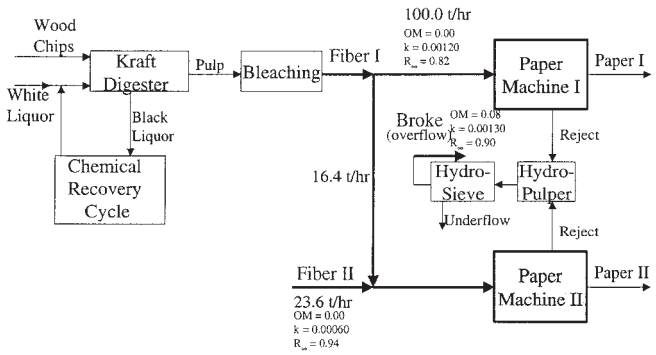

Figure 10. Pulp and paper process.

sodium hydroxide and sodium sulfide as the main active ingredients). The spent solution (black liquor) is converted back to white liquor via a recovery cycle (evaporation, burning, and causticization). The digested pulp is passed to a bleaching system to produce bleached pulp (fiber I). The plant also purchases an external pulp (fiber II). Two types of paper are produced through two papermaking machines (sinks I and II). Paper machine I employs 100 tons/h of fiber I. However, a mixture of fibers I and II (16.4 and 23.6 tons/h, respectively) is fed to paper machine II. As a result of processing flaws and interruptions, a certain amount of partly and completely manufactured paper is rejected. These waste fibers are referred to as broke. The reject is typically passed through a hydro-pulper and a hydro-sieve with the net result of producing an underflow, which is burnt, and an overflow of broke which goes to waste treatment. It is worth noting that the broke contains fibers that may be partially recycled for papermaking.

The case study is aimed at providing optimal solutions to the following design questions:

(a) Direct Recycle and Reallocation: What is the optimal allocation of the three fiber sources (fiber I, fiber II, and broke) for a direct recycle/reuse situation (no new equipment)?

(b) Interception of Broke: To maximize the use of process resources and minimize wasteful discharge (broke), how should the properties of broke be altered so as to achieve its maximum recycle?

The performance of the paper machines and, consequently, the quality of the produced papers rely on three primary properties (Biermann, 1996; Brandon, 1981; Willets, 1958):

- **Objectionable material (*OM*)**: this refers to the undesired species in the fiber (expressed as mass fraction).
- **Reflectivity (R_∞)**: which is defined as the reflectance of an infinitely thick material compared to an absolute standard, which is Magnesium Oxide (MgO).
- **Absorption Coefficient (k):** which is an intensive property that provides a measure of absorptivity of light into the fibers (black paper has a high value of k). Hemicellulose and cellulose have very little absorption of light in the visible region.

However, lignin has a high absorbance. Therefore, light absorbance is mostly attributed to lignin. The light absorption coefficient is a very useful property in determining the opacity of the fibers. Opacity ($C_{0.89}$) is defined as the ratio of reflectance of a single sheet, which is backed by a black body, compared to a sheet that is backed by a white body at 89% reflectance. Values and relationships of opacity, reflectivity, and the adsorption coefficient can be determined using the Kubelka-Munk theory (for example, Biermann, 1996), which relates the basis weight of paper, opacity, and reflectivity of paper to one another.

The mixing rules for OM and k are linear (Brandon; 1981), that is

$$\overline{OM} = \sum_{s=1}^{N_s} x_s.OM_s \tag{50}$$

$$\bar{k}\left(\frac{m^2}{g}\right) = \sum_{s=1}^{N_s} x_s k_s\left(\frac{m^2}{g}\right) \tag{51}$$

However, a nonlinear empirical mixing rule for R_∞ is developed using data from Willets (1958)

$$\bar{R}_\infty^{5.92} = \sum_{s=1}^{N_s} x_s R_{\infty_s}^{5.92} \tag{52}$$

Tables 2 and 3 describe the constraints for the two sinks, while Table 4 provides the data on the properties of the sources.

Table 2. Constraints for Paper Machine I (Sink I)

Property	Lower Bound	Upper Bound
OM (mass fraction)	0.00	0.02
k (m^2/gm)	0.00115	0.00125
R_∞	0.80	0.90
Flow rate (ton/hr)	100	105

Table 3. Constraints for Paper Machine II (Sink II)

Property	Lower Bound	Upper Bound
OM (mass fraction)	0.00	0.00
k (m^2/gm)	0.00070	0.00125
R_∞	0.85	0.90
Flow rate (ton/hr)	40	40

Solution

To transform the problem from the property domain to the cluster domain, let us arbitrarily select the following reference values of the raw properties:

$$OM^{ref} = 0.01 \tag{53a}$$

Table 4. Properties of Fiber Sources

Source	OM (Mass Fraction)	k (m^2/gm)	R_∞	Maximum Available Flow Rate (ton/hr)	Cost ($/ton)
Broke	0.08	0.00130	0.90	30	0
Fiber I	0.00	0.00120	0.82	∞	210
Fiber II	0.00	0.00060	0.94	∞	400

$$k^{\text{ref}} = 0.001 \text{ m}^2/\text{gm} \tag{53b}$$

$$R_{\infty}^{\text{ref}} = 1.0 \tag{53c}$$

First, we use the values of the properties for the three usable sources (broke, fiber I and, fiber II) from Table 4 and map them to the cluster domain. Similarly, the sink constraints defined by Tables 2 and 3 are transformed into feasibility regions on the ternary cluster diagram. The rules derived in Table 1 illustrate the six points defining the BFR. For instance for sink I, those values are summarized in Table 5.

Figure 11 shows the results. While the feasibility region for sink I is a two-dimensional (2-D) zone, it is a line segments for sink II as it lies on the zero cluster line for the objectionable materials (the base of the triangle).

As has been mentioned in the theoretical analysis (Eqs. 41–43), each cluster point within the feasibility region of the sink may correspond to multiple combinations of property points. For each property combination, the corresponding augmented property index is calculated. For instance, the range for the values of *AUP* shown in Figure 12 refer to the interval designating [Argmin AUP_m, Argmax AUP_m]. Figure 12 shows these intervals for selected points, primarily on the boundaries of the feasibility region of the sink because of the importance that boundary points play according to the visualization tools based on Rule No. 2. For instance, the cluster point (C_{OM} = 0.56, C_k = 0.34, C_R = 0.10) corresponds to multiple combinations of feasible properties that yield this value of the cluster. As an example, let us consider two property combinations: (OM = 0.01877, k = 0.00115, R_{∞} = 0.83475) and (OM = 0.02000, k = 0.001225, R_{∞} = 0.84371). Both yield the same value of the cluster (C_{OM} = 0.557, C_k = 0.341, C_R = 0.102), but the first one has an *AUP* of 3.37, while the second one has an *AUP* of 3.59.

With the mapping of the problem data from the property domain to the cluster domain completed, we can now readily solve the property integration problem.

Our first objective is to maximize the recycle of broke since

Table 5. Vertices of the BFR for Sink I

Characteristic Dimensionless Operators	Corresponding Values of Raw Properties	Corresponding Values of Clusters	AUP_{Sink}
$(\Omega_{i,s}^{\min}, \Omega_{j,s}^{\max}, \Omega_{k,s}^{\min})$	0.00	0.00	1.69
	0.90	0.32	
	0.00115	0.68	
$(\Omega_{i,s}^{\min}, \Omega_{j,s}^{\max}, \Omega_{k,s}^{\max})$	0.00	0.00	1.79
	0.90	0.30	
	0.00125	0.70	
$(\Omega_{i,s}^{\min}, \Omega_{j,s}^{\min}, \Omega_{k,s}^{\max})$	0.00	0.00	1.52
	0.80	0.18	
	0.00125	0.82	
$(\Omega_{i,s}^{\max}, \Omega_{j,s}^{\min}, \Omega_{k,s}^{\max})$	0.02	0.57	3.52
	0.80	0.07	
	0.00125	0.36	
$(\Omega_{i,s}^{\max}, \Omega_{j,s}^{\min}, \Omega_{k,s}^{\min})$	0.02	0.58	3.42
	0.80	0.08	
	0.00115	0.34	
$(\Omega_{i,s}^{\max}, \Omega_{j,s}^{\max}, \Omega_{k,s}^{\min})$	0.02	0.54	3.69
	0.90	0.15	
	0.00115	0.31	

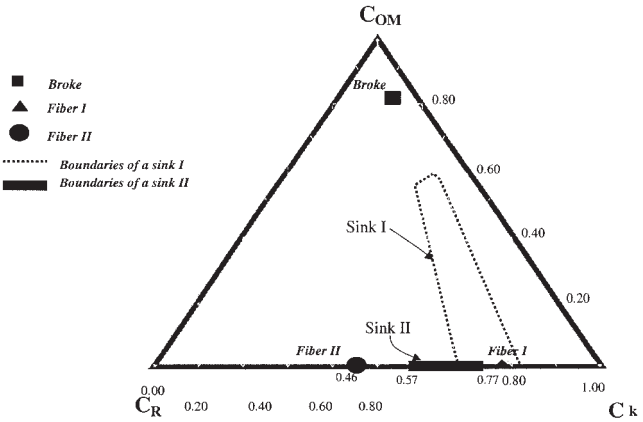

Figure 11. Three usable sources and the feasibility regions for Sinks I and II.

it is the internal source (process stream for free). Any mixture of broke, fiber I and fiber II is contained in the triangle connecting the three sources. Let us start with sink I. From Figure 12, it can be seen that the optimum mixing point is the intersection of the broke-fiber I line with the feasibility region of sink I. This optimal mixing point, whose coordinates are (C_{OM} = 0.56, C_k = 0.34, C_R = 0.10), provides the longest relative arm for the broke and the shortest relative arm for fiber I. The cluster coordinates for the broke are (C_{OM} = 0.81, C_k = 0.13, C_R = 0.06) with an AUP_{broke} of 9.84. The value of $AUP_{\text{Fiber I}}$ is 1.51. Hence, Eq. 49b applies and for $AUP_{\text{Sink I@}(C_{\text{OM}}=0.56, C_k=0.34, C_R=0.10)}$ = 3.59, the relative arm for fiber I can be calculated from the graph

$$\beta_{\text{Fiber I}} = \frac{\text{Arm for Fiber I}}{\text{Total arm connecting broke to Fiber I}} \tag{54}$$

These arms can be measured from the graph. Equivalently, we can use one of the cluster coordinates based on Eq. 8. Hence

$$\beta_{\text{Fiber I}} = \frac{0.81 - 0.56}{0.81 - 0.00} = 0.31 \tag{55}$$

Hence, according to Eq. 6

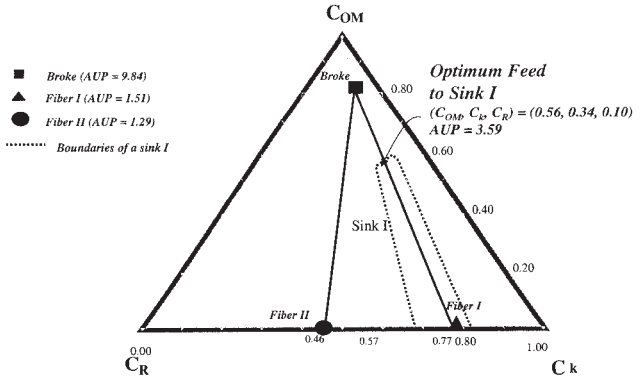

Figure 12. Optimal mixing point for Sink I.

$$x_{\text{Fiber I}} = \frac{3.59}{1.51}(0.31) = 0.74 \tag{56}$$

Alternatively, Eq. 47 can be used to calculate $x_{\text{Fiber I}}$

$$x_{\text{Fiber I}} = \frac{3.59 - 9.84}{1.51 - 9.84} = 0.75 \tag{57}$$

The slight discrepancy between the calculated values of Eqs. 56 and 57 is within the accuracy of reading from the ternary diagram.

Using the value of the fractional contribution of fiber I from Eq. 57, and for a total flow rate of 100.0 tons/h fed to sink I, we get

$$\text{Optimum flow rate of Fiber I} = 0.75 * 100 = 75.0 \text{ tons/hr} \tag{58}$$

and through material balance around sink I, the flow rate of recycled broke can be obtained

$$\text{Maximum flow rate of directly recycled broke} = 100.0 - 75.0 = 25.0 \text{ tons/hr} \tag{59}$$

We can now map the cluster of the optimal mixing point back to the property domain. For the optimal mixing point, whose coordinates are ($C_{OM} = 0.56$, $C_k = 0.34$, $C_R = 0.10$), and whose AUP is 3.59, we can use the clustering equations to back calculate the equivalent properties to be

$$OM_{Sink\ I} = 0.02 \tag{60a}$$

$$k_{\text{Sink I}} = 0.001225 \text{ m}^2/\text{gm} \tag{60b}$$

$$R_{\infty,\text{Sink I}} = 0.844 \tag{60c}$$

Next, we proceed to sink II. Since the boundaries for this sink lie on the zero-OM cluster line (Figure 12), no broke can be recycled to the sink, and the only feasible mixture is between fibers I and II. The values of the augmented property indices for fibers I and II are $AUP_{\text{Fiber I}} = 1.51$ and $AUP_{\text{Fiber II}} = 1.29$. Since fiber II is more expensive than fiber I, but $AUP_{\text{Fiber I}} > AUP_{\text{Fiber II}}$, then Eq. 49b applies and we should select the highest feasible value for $AUP_{\text{Sink II}}$ at the optimum mixing point. Therefore, we start with the shortest arm for fiber II (as close as possible to the cluster location of fiber I). As can be seen from Figure 13, the AUP range for sink II at the shortest arm (at C_k =0.77) is [1.63, 1.63] which is higher than either AUP for fibers I and II. Therefore, there can be no feasible mixture of fibers I and II that matches the AUP of the sink at that point. Therefore, we systematically increase the arm of fiber II (that is, we move to the left closer to fiber II), and for each feasible mixing point we start with Argmax AUPsink II and keep decreasing till we get a feasible answer. Hence, the optimum answer is the one shown in Figure 13, with coordinates of $C_{OM} = 0.00$, $C_k = 0.74$, $C_R = 0.26$, and an AUP of 1.47.

The relative arm for fiber II can be calculated from the graph

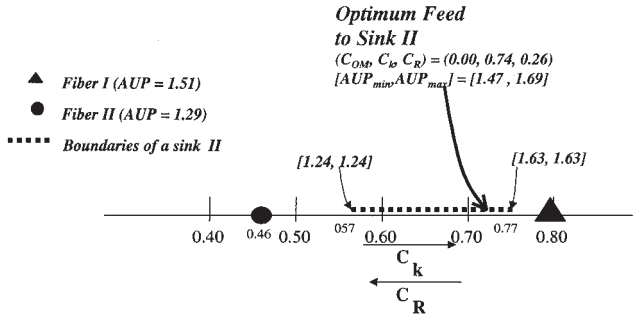

Figure 13. Optimal mixing point for Sink II (two numbers inside each bracket correspond to minimum and maximum values of AUP at the cluster point).

$$\beta_{\text{Fiber II}} = \frac{\text{Arm for Fiber II}}{\text{Total arm connecting Fiber II to Fiber I}} \tag{61}$$

These arms can be measured from the graph leading to

$$\beta_{\text{Fiber II}} = \frac{0.80 - 0.74}{0.80 - 0.46} = 0.17 \tag{62}$$

Hence, according to Eq. 6

$$x_{\text{Fiber II}} = \frac{1.47}{1.29}(0.17) = 0.19 \tag{63}$$

Alternatively, Eq. 47 can be used to calculate $x_{\text{Fiber II}}$

$$x_{\text{Fiber II}} = \frac{1.47 - 1.51}{1.29 - 1.51} = 0.18 \tag{64}$$

Again, the slight discrepancy between the calculated values of Eqs. 63 and 64, is within the accuracy of reading from the ternary diagram.

Based on the definition of fractional contribution, and the value of fractional contribution of fiber II from Eq. 63, and a total flow rate of 40.0 tons/h fed to sink II, we get

$$\text{Optimum flow rate of Fiber II} = 0.19 * 40 = 7.6 \text{ tons/hr} \tag{65}$$

through material balance around sink II, the flow rate of fiber I can be obtained

$$\text{Optimum flow rate of Fiber I} = 40.0 - 7.6 = 32.4 \text{ tons/hr} \tag{66}$$

We can now map the cluster of the optimal mixing point back to the property domain. For the optimal mixing point, whose coordinates are ($C_{OM} = 0.00$, $C_k = 0.74$, $C_R = 0.26$), and whose AUP is 1.47, we can use the clustering equations to back calculate the equivalent properties to be

$$OM_{Sink\ II} = 0.00 \tag{67a}$$

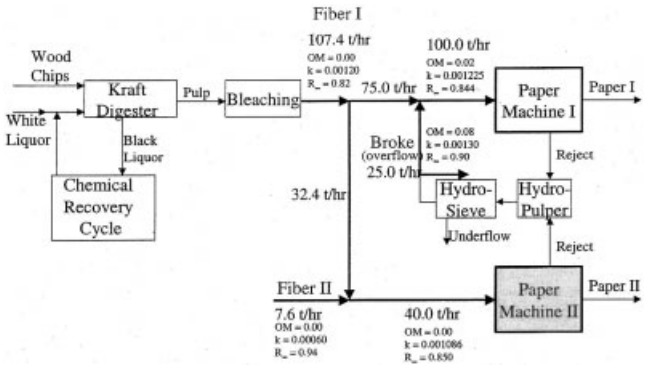

Figure 14. Optimum direct-recycle solution.

$$k_{\text{Sink II}} = 0.001086\ \text{m}^2/\text{gm} \tag{67b}$$

$$R_{\infty,\text{Sink II}} = 0.850 \tag{67c}$$

The optimum direct-recycle and reallocation of sources solution is shown in Figure 14. It illustrates the revised flow rates of the sources and the new properties entering the sinks. It is useful to compare the cost of raw materials before and after recycle.

The initial cost of raw materials before recycle/reallocation

$$= 116.4\ \text{tons of Fiber I} * \$210/\text{ton} + 23.6\ \text{tons of Fiber II} * \$400/\text{ton} = \$33{,}884/\text{hr} \tag{68}$$

The cost of raw materials after recycle/reallocation

$$= 107.4\ \text{tons of Fiber I} * \$210/\text{ton} + 7.6\ \text{tons of Fiber II} * \$400/\text{ton} = \$25{,}594/\text{hr} \tag{69}$$

Therefore, direct recycle and reallocation of sources results in a 24.5% reduction in cost of raw materials.

Solution to part b

Part b deals with the interception of the broke. To maximize the use of process resources (broke), how should the properties of broke be altered so as to achieve its maximum recycle?

As can be seen from Figure 7, once a mixing point is selected, one can determine the minimum extent of interception to adjust the properties of the broke. Multiple candidate mixing points can be selected as mentioned earlier (Figures 7 and 8). For instance, let us select the same mixing point as in the case of direct recycle. The coordinates for the selected mixing point are $C_{OM} = 0.56$, $C_k = 0.34$, $C_R = 0.10$, and the optimum AUP of the sink is 3.59. Maximum recycle of broke is the total recycle, that is, 30 tons/h. Hence, minimum usage of fiber I in sink I is 70 tons/h leading to a fractional contribution of

$$x_{\text{Fiber I}} = 70/100 = 0.70 \tag{70}$$

Recalling that $AUP_{\text{Fiber I}} = 1.51$ and substituting this value and Eq. 70 into Eq. 6, we get

$$\beta_{\text{Fiber I}} = \frac{0.70}{3.59}(1.51) = 0.29 \tag{71}$$

However, the relative arm for fiber I is defined as

$$\beta_{\text{Fiber I}} = \frac{\text{Arm for Fiber I}}{\text{Total arm connecting intercepted broke to Fiber I}} \tag{72}$$

These arms can be measured from the graph. Equivalently, one can use the cluster coordinates based on Eq. 8. Hence

$$\beta_{\text{Fiber I}} = \frac{C_{\text{OM}}^{\text{Intercepted}} - 0.56}{C_{\text{OM}}^{\text{Intercepted}} - 0.00} \tag{73}$$

Equating Eqs. 72 and 73, we get

$$C_{OM}^{\text{Intercepted}} = 0.79 \tag{74}$$

Similarly

$$\beta_{\text{Fiber I}} = \frac{C_k^{\text{Intercepted}} - 0.34}{C_k^{\text{Intercepted}} - 0.80} = 0.29 \rightarrow C_k^{\text{Intercepted}} = 0.15 \tag{75}$$

and, according to Eq. 5

$$C_R^{\text{Intercepted}} = 0.06 \tag{76}$$

Using Eq. 46a, we get

$$3.59 = 0.7 * 1.51 + 0.3 * AUP_{\text{broke}}^{\text{Intercepted}} \rightarrow AUP_{\text{broke}}^{\text{Intercepted}} = 8.44 \tag{77}$$

Therefore, the minimum interception task entails bringing the broke to an intercepted cluster point of (0.79, 0.15, 0.06) and an $AUP_{\text{broke}}^{\text{Intercepted}} = 8.44$. Using the clustering equations to map back to the property domain for the intercepted broke, we get

$$OM^{\text{Intercepted}} = 0.067 \tag{78a}$$

$$k^{\text{Intercepted}} = 0.0013\text{m}^2/\text{gm} \tag{78b}$$

$$R_{\infty}^{\text{Intercepted}} = 0.90 \tag{78c}$$

This analysis has identified the minimum interception task for the broke without committing to the specific nature of the interception device. Later, conventional process synthesis techniques can be used to screen candidate interception techniques and to select optimum system. In essence, we have targeted for the performance of the interception device. This is an important linkage between property integration and process synthesis. It is worth pointing out that the same procedure can be carried out for other mixing points or for the second sink.

Figure 15 shows the interception task for the broke stream

while Figure 16 represents the revised flowsheet following interception and reallocation.

The cost of raw materials after interception and reallocation = 102.4 tons of fiber I

$$*\$210/\text{ton} + 7.6 \text{ tons of Fiber II} * \$400/\text{ton} = \$24{,}544/\text{hr} \tag{79}$$

Therefore, direct recycle and reallocation of sources results in a 27.6% reduction from the initial cost of raw materials.

Conclusions

This work has introduced the general problem of property integration, derived mathematical expressions for its optimal strategies, and presented systematic techniques for its graphical solution. The main idea is to carry out the design not based on chemical components, but instead based on integrating the properties of sources to sinks and adjusting properties using interception devices. The property integration problem has been mapped into a dual representation on the cluster domain. Trigonometric techniques have been used to identify the exact shape of the feasibility region in the cluster domain *a priori,* and without the need to map infinite points from the property domain to the cluster domain. Optimization rules have been derived to relate cost to fractional contributions and fractional contributions to cluster arms. Next, graphical tools have been developed to determines optimum allocation strategies and minimum extent of needed interception. Furthermore, the article has presented a systematic way of dealing with multiple mappings from the primal domain (properties) to the dual representation (ternary clusters). Criteria for the selection of augmented property index have been developed to define the optimal solution from among the multiple feasible solutions at the same cluster point. A case study has been solved on fiber recovery and resource conservation for papermaking. In addition, to the practical aspects associated with the developed procedure, the devised representation and tools provide a unique and insightful perspective on the key characteristics of the process that are not apparent from the property domain. The developed framework can be used as the basis for many novel contributions in the areas of process synthesis and molecular design.

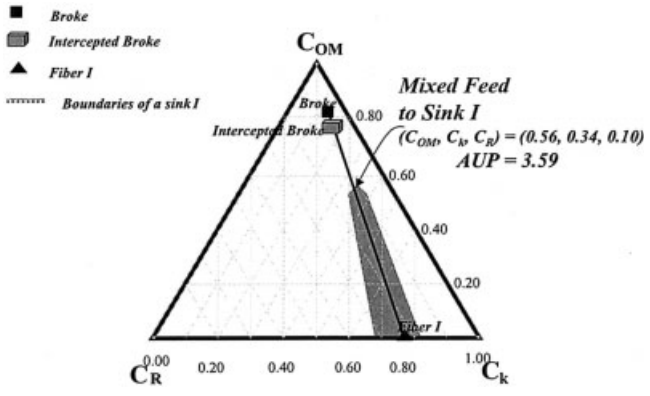

Figure 15. Determination of the minimum extent of interception for the broke.

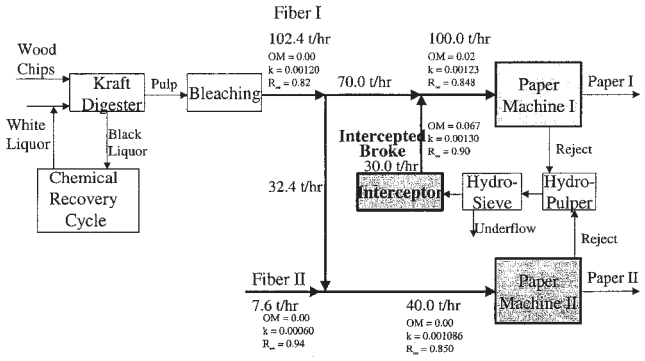

Figure 16. Optimal solution with interception and reallocation.

Acknowledgment

The authors are grateful for the help provided by Dr. Gopal Krishnagopalan and Dr. Mark Shelley. Funding from the U.S. EPA Gulf Coast Hazardous Substances Research Center is gratefully acknowledged.

Notation

$Argmax$ = highest value of an element in a set
$Argmin$ = lowest value of an element in a set
AUP = augmented property index as defined by Eq. 3
AUP_m = augmented property index for point m in a sink
AUP_s = augmented property index for source s
$\overline{AUP}$ = augmented property index of mixture
C = cluster
$C_{i,s}$ = cluster of property i in source s as defined by Eq. 4
$\bar{C}$ = cluster of mixing
$C_{0.89}$ = TAPPI opacity
$Cost_s$ = cost of source s, \$/ton
$Cost_{mixture}$ = cost of mixture, \$/ton
F_s = flow rate of source s, tons/h
i = index for raw properties or surrogate clusters
$INTERVAL\_AUP_m$ = the interval bounding the range for the AUP at sink point m as defined by Eq. 43
j = index for sinks
k = absorption coefficient
m = a feasible point satisfying sink constraints
$n_{Multiple}$ = number of multiple property points leading to the same value of the cluster
N_c = number of clusters
N_s = number of sources
p_i = i^{th} property
$p_{i,m}$ = i^{th} property for point m in the sink
$R_{0.89}$ = reflectance of a single sheet backed by white body
R_∞ = reflectivity
s = index for sources (streams)
$SET\_AUP^{\text{Feasible}}_{(C_1^{\text{sink}}, C_2^{\text{sink}}, C_3^{\text{sink}})}$ = set of all feasible AUP's for property combinations yielding the same value of clusters (C_1^{sink}, C_2^{sink}, C_3^{sink})
W = internal process stream
x_s = fractional contribution of the s^{th} stream into the total flowrate of the mixture

Subscripts

k = absorption coefficient
m = a feasible point satisfying sink constraints
OM = objectionable materials
R = reflectivity

Superscripts

Feasible = a feasible point in a sink
int = intercepted value
ref = reference value

Greek letters

β_s = mixing arm of stream s on the ternary cluster diagram
ψ_i = operator used in the mixing formula for the i^{th} property as defined by Eq. 1
$\Omega_{i,s}$ = normalized, dimensionless operator for the i^{th} property of the s^{th} source as defined by Eq. 2

Literature Cited

Biermann, C. J., *Handbook of Pulping and Papermaking*, Academic Press, San Diego, CA, pp 32–40, 158–159, 193–208, 251–252, 502–515 (1996).

Brandon, C. E., "Properties of Paper," *Pulp and Paper Chemistry and Chemical Technology*, 3rd ed., Vol. 3, James P. Casey, ed., Wiley, New York, pp 1739–1746, 1819–1886 (1981)

El-Halwagi, M. M., *Pollution Prevention through Process Integration Systematic Design Tools,* Academic Press, San Diego, CA, pp 1–190, 217–247 (1997),

El-Halwagi, M. M., and H. D. Spriggs, "Solve Design Puzzles with Mass Integration", *Chem. Eng. Prog.*, **94**, 25 (1998)

Linnhoff, B., D. W. Townsend, D. Boland, G.F. Hewitt, B. E. A. Thomas, A. R. Guy, and R.H. Marsland, *A User Guide to Process Integration for the Efficient Use of Energy*, Revised 1st ed., Inst. of Chem. Eng., Rugby, U.K. (1994).

Shelley, M. D., and M. M. El-Halwagi, "Component-Less Design of Recovery and Allocation Systems: a Functionality-Based Clustering Approach," *Computers. and Chem. Eng.*, **24**, 2081 (2000).

Willets, W. R., "Titanium Pigments," *Paper Loading Materials*, TAPPI Monograph Series - No. 19, Technical Association of the Pulp and Paper Industry, New York, NY, pp 96–114 (1958).

Manuscript received Apr. 26, 2002, revision received Jun 26, 2003, and final revision received May 27, 2004.